MAGNETIC AND PHOTOLUMINESCENCE PROPERTIES OF GLASSES $AgCl–Ga_2S_3–La_2S_3: Er_2S_3$.

Halyan V.V.[1], Krasnovyd S.V. [2*], Konchits A. A.[2], Shanina B. D.[2], Zhuchenko Z.[2], Vorona I. P.[2], Yukhymchuk V. O. [2], Bodnaruk A. V.[3], Povarchuk V.Yu. [3]
[1]*Lesya Ukrainka Volyn National University, Lutsk, Ukraine*
[2]*V. Lashkaryov Institute of Semiconductor Physics, NAS of Ukraine, Kyiv, Ukraine*
[3]*Institute of Physics, NAS of Ukraine, Kyiv, Ukraine*
**sergkrasnovyd88@gmail.com*

Among the wide variety of semiconductor structures intensively studied in the last decade, crystalline and glassy chalcogenides occupy an important place. The uniqueness of these materials lies in their high transparency in the visible and IR ranges, their inherent high refractive index, resistivity to aggressive media, high solubility of rare-earth metals (REM) in them, and sensitivity to external factors, in particular laser, electron- and γ-irradiation, magnetic field, temperature, etc. It has been established, in particular, that γ-irradiation of chalcogenide glasses generates many defects and significantly affects their photoluminescent characteristics [1].

In recent years, gallium and lanthanum-based chalcogenides have attracted particular attention because, along with the above-mentioned high properties, they have relatively simple technology, low cost, thermal stability, and non-toxicity. Moreover, it is found that the presence of two types of lanthanides (La and Er) in glass allows for the implementation of new luminescence schemes, but their mechanisms and the origin of additional bands are still not sufficiently studied [2].

In this work, the magnetic, magnetic resonance, and photoluminescent properties of $AgCl–Ga_2S_3–La_2S_3: Er_2S_3$ glasses with different erbium concentrations were studied. Alloys for glasses of the La2S3-Er2S3-Ga2S3 system with a sample weight of 2 g were presynthesized at a temperature of 870 K and a holding time of 24 h. The obtained samples were crushed and loaded into quartz containers. After two-stage stepwise heating and subsequent 3-hour holding at a T=1420 K, the samples were quenched in a saturated NaCl solution with crushed ice [3]. The composition samples are provided in Table 1. Samples S0 and S1 were not irradiated, while samples S2 to S7 were irradiated with a high-energy electron beam with a dose of 50 kGy.

Table 1. Composition of the studied samples

Sample	Composition, mol.%			
	La_2S_3	Ga_2S_3	AgCl	Er_2S_3
S0	30	66	4	0
S1	30	63	4	3
S2	30	66	4	0
S3	30	68.75	1	0.25
S4	30	67.5	2	0.5
S5	30	66.25	3	0.75
S6	30	65	4	1
S7	30	63	4	3

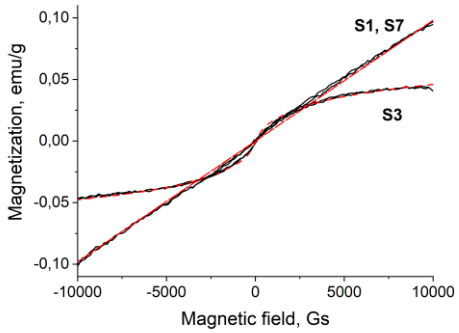

Fig. 1. Magnetization curves for the most representative samples S1,S7, and S3. Solid and dashed lines are the experimental and the theoretical simulation.

Magnetization σ (H) measurements were conducted at T = 300 K for all samples with different compositions. Most of the samples show superparamagnetic (SPM) properties due to the presence of magnetic clusters (curve S3 in Fig. 1). The Langevin function describes the $\sigma_{SPM}(H)$:

$$\sigma_{SPM}(H)=n\mu\cdot L(\mu H/kT)=n\mu\cdot(\coth(\mu H/kT)-kT/\mu H) \quad (1)$$

Where μ is the average magnetic moment of an SPM particle, n is the number of SPM particles, and H is the external magnetic field. It was found that among all samples, sample S3 has the highest concentration of small superparamagnetic clusters. In contrast, samples S1 and

S7 demonstrate only paramagnetic properties $\sigma_{PC}(H)=\chi_{PC}\cdot H$ (curves S1, S7 in Fig. 1), where $\sigma_{PC}(H)$ is given in emu/g, $\chi_{PC}=N\mu_B^2g^2/4/kT/\rho$; ρ is the density of the glass sample, N is the concentration of paramagnetic centers (PC).

Analysis of the obtained data regarding the properties of superparamagnetic contributions to magnetic resonance signals clearly shows that the intensity of clustering processes in glass samples decreases with increasing erbium concentration, and at 3 mol.% Er, they are practically absent. In addition, in samples with a high erbium content, the magnetic properties do not depend on electron irradiation (compare curves S1 and S7 in Fig. 1).

Magnetic resonance spectra of several samples at T=300 K are shown in Fig. 2.

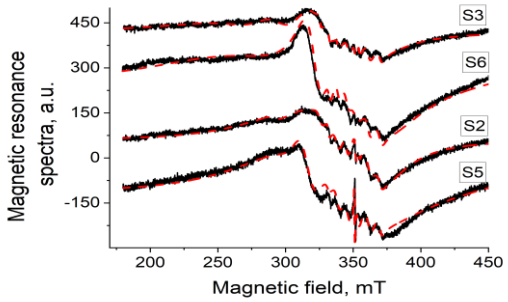

Fig. 2. Spectra of the magnetic resonance for samples S3, S6, S2, S5, recorded as the derivative of absorption over magnetic field. Black solid lines are the experimental, red dashed lines are the theoretical simulation results.

It was established that each of the spectra observed in Fig. 2 is the sum of four resonance signals: one superparamagnetic signal and three electron paramagnetic resonance (EPR) signals. Taking into account the fact that magnetic resonance signals of Er^{3+} ions are not observed at room temperatures due to fast spin relaxation processes, we conclude that the superparamagnetic contribution to the magnetic resonance spectra is due to the same SPM clusters as in the

magnetization experiments. The description of the SPM signals was carried out within the framework of a model that takes into account the hexagonal crystal structure for the initial components (La_2S_3, Ga_2S_3, Er_2S_3) and is disordered in a glass form, the anisotropy constant and demagnetization field are treated as axial functions. The origin of superparamagnetic signals is most likely related to the aggregation of La_2S_3.

One of the EPR signals is manifested as a set of hyperfine lines due to the hyperfine interaction between the electron spin (S=1/2) and the nuclear spin (I=7/2). The paramagnetic centers with a g-factor with small variations around the value 1.98 should be related to the sulfur dangling bonds Ga-S, as previously revealed for the dichalcogenide MoS_2 [4]. Two other signals can also be ascribed to the sulfur dangling bond, which shifts to the low field due to dipole-dipole interaction with SPM particles.

The most intriguing result of this work is the first correlation discovered between the structural disorder of glasses, manifested in the formation of a significant concentration of superparamagnetic clusters of various sizes, on the one hand, and the features of the photoluminescent properties of such samples, on the other hand. Fig. 3 shows the PL spectra of several studied glass samples.

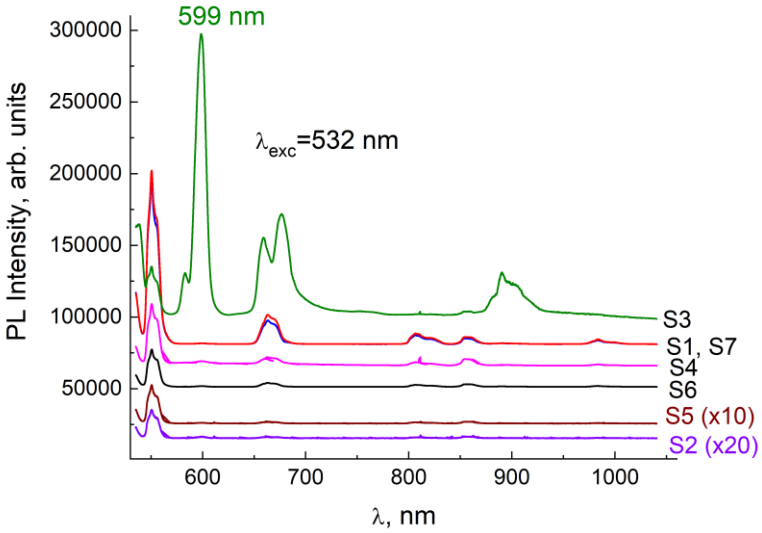

Fig. 3. Photoluminescence spectra of some glass samples. The amplitudes of the PL signals are not fully correlated with each other due to the need to use optical filters (HC9, HC11) with different transmission capacities, which are determined with some error.

It is evident from the spectra in Fig. 3 that, along with the 550 nm PL band, the intensity of which is highest in the samples with the highest erbium concentration (samples S1 and S7), a new, intense band at 599 nm is recorded in sample S3 with the highest concentration of superparamagnetic clusters. Its nature is currently being studied. Note that in Ref. [2], a 663 nm PL band was observed, the appearance of which was associated with a two-stage process: 1) Transfer of electrons from the conduction band to the valence band of La_2S_3. 2) Transition of an electron to the $^4F_{9/2}$ level with subsequent radiative recombination between the $^4F_{9/2}$ and $^4I_{15/2}$ levels.

Finally, in this work, magnetic properties, including magnetic resonance characteristics of La and Er containing glasses, were determined, and their correlation with photoluminescent properties of samples was established. Results obtained open up new possibilities for the formation of magnetic and luminescent characteristics of materials with specified properties.

References:

1. V.V. Halyan, A.A. Konchits, B.D. Shanina, et.al. EPR of γ -induced defects and their effects on the photoluminescence in the glasses of the $Ag_{0.05}$ $Ga_{0.05}$ $Ge_{0.95}S_2$ $-Er_2S_3$ system. Radiation Physics and Chemistry 115 (2015) 189–195.
2. Guillaume Gouget, Morgane Pellerin, Rabih Al Rahal Al Orabi, et. al. Rare-Earth Sulfide Nanocrystals from Wet Colloidal Synthesis: Tunable Compositions, Size-Dependent Light Absorption, and Sensitized Rare-Earth Luminescence. J. Am. Chem. Soc. 2021, 143, 3300 – 3305.
3. I.V. Kityk, V.V. Halyan, V.O. Yukhymchuk, at.al. NIR and visible luminescence features of erbium doped Ga_2S3 – La_2S_3 glasses. J. Non Cryst Solids. 2018. Vol. 498. P. 380–385.
4. Lei Li, Zhaodan Qin, Lucie Ries, et al. Role of Sulfur Vacancies and Undercoordinated Mo Regions in MoS_2 Nanosheets toward the Evolution of Hydrogen. J. Am. Chem. Soc., 2019, 13, 6824−6834, DOI: 10.1021/jacsnano.9b01583

MULTISPECTRAL LIDAR SYSTEMS AND THEIR APPLICATIONS

Mashevskyi Igor, Myronchuk Galyna, Migalska-Zalas Anna

Lesya Ukrainka Volyn National University, Ukraine; Jan Dlugosz University in Czestochowa, Poland
igor.mashevskyi@vnu.edu.ua

The abstract highlights the principles of multispectral LiDAR (MSL) system design, implementation strategies for data collection and processing, and major avenues for real-world deployment. MSL systems incorporate laser emitters operating at different wavelengths, scanning and receiving optical components, photodetectors, and satellite positioning modules (GPS/IMU), enabling the capture of spatial and spectral data simultaneously with high precision. One of the core strengths of MSL is its capability to measure distances and record reflected signal intensity across several wavelengths, enhancing material differentiation and classification.

Techniques such as the application of supercontinuum lasers and frequency doubling are discussed for spectral range expansion. MSL configurations can rely on multiple discrete laser sources or broadband laser systems combined with wavelength-selective optics. Key data processing methods include radiometric calibration, atmospheric compensation, and artificial intelligence approaches for analysis, segmentation, classification, and visual interpretation of 3D spectral point clouds.

Application domains include precision agriculture (crop health and stress analysis), environmental and ecological monitoring, forestry inventory (canopy and biomass analysis), high-resolution topographic mapping, infrastructure diagnostics in urban planning, geological exploration (mineral composition and structural integrity), and archaeological site discovery. Recent market analyses reflect an increasing demand for MSL-based technologies and their integration within sensor fusion platforms.

It is concluded that MSL represents a next-generation remote sensing solution for accurate, large-scale, and non-destructive environmental assessment and monitoring, supporting innovation across research and industry.

1. Wasser L. A. (2024). The Basics of LiDAR - Light Detection and Ranging. NSF NEON.
2. Takhtkeshha N., Mandlburger G., Remondino F., Hyyppä J. (2024). Multispectral LiDAR Technology and Applications: A Review. Sensors, 24(5), 1669.
3. Gong W. et al. (2015). Object Classification with Multispectral LiDAR Data. Sensors, 15(9), 21989–22002.